J. Geophys. 44, 511–523, 1978

Journal of Geophysics

Digital Recording and Analysis of Broad-Band Seismic Data at the Graefenberg (GRF)-Array

H.-P. Harjes and D. Seidl

Seismologisches Zentralobservatorium Gräfenberg, Krankenhausstraße 1–3, 8520 Erlangen, Federal Republic of Germany

Abstract. An array of 19 broad-band seismometers with flat velocity response between 0.05 Hz and 5 Hz combined with a binary gain-ranging data acquisition system of 138 db dynamic range is being installed in Southern Germany. The array has a maximum extension of 80 km, it consists mainly of three triangular subarrays, the dimensions of which are chosen so as to reduce the microseisms by simple summation. The dynamic range is accomplished by digitizing the output at the seismometer sites and transmitting the digital information on telephone lines to a central control station. Single station data are available since 1975 and continuous recordings of the first subarray exist since 1976. They provide extended information of the fine structure of the seismic wave field in the medium frequency range between 0.5 Hz and 0.05 Hz and allow the quantitative investigation of frequency-dependent seismic phenomena over a wide range of amplitude and frequency. An elementary problem is the numerical analysis of broad-band seismograph systems especially seismometer-galvanometer systems and the determination of the true ground displacement or velocity. This simulation and restitution problem can be solved by digital recursive filters applying the z-form method. The simulation may include high sensitive short-period detection instruments.

Key words: GRF-array – Broad-band seismology – Digital seismogram analysis.

Introduction

A broad-band array is in the process of being installed at the Graefenberg-Observatory (GRF) in Southern Germany, which is the Central Seismological Observatory of the Federal Republic of Germany. This set-up and especially the new array concept is a joint project of the seismological institutions of our country.

The idea of establishing an array was to provide different seismic groups

0340-062X/78/0044/0511/$02.60

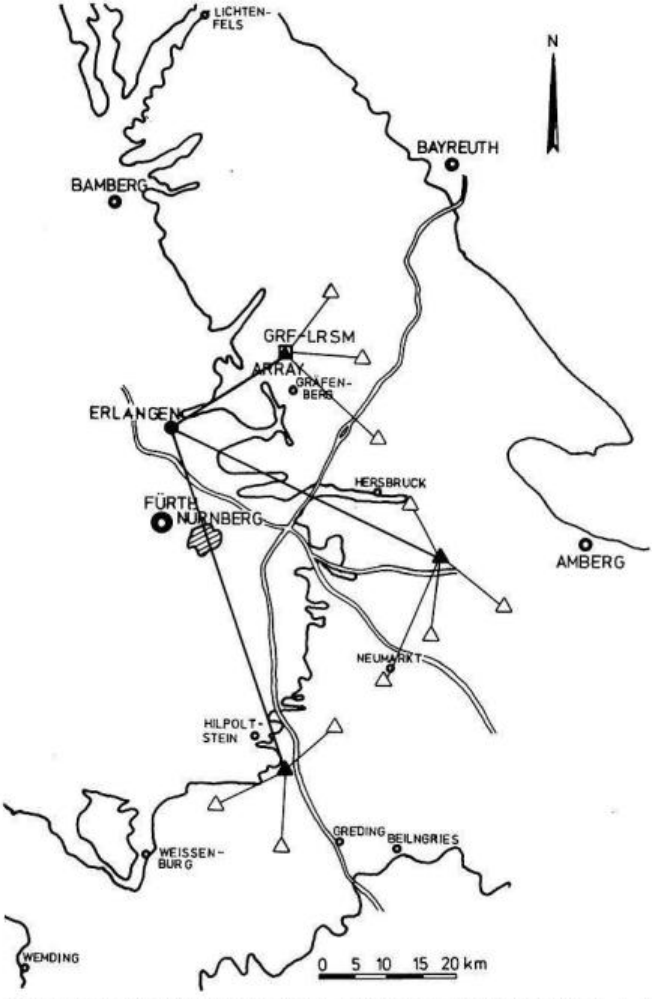

Fig. 1. Map showing the location of GRF broad-band array. ▲ Three-component station and subarray center; △ Single-component station (vertical seismometer); □ GRF LRSM-array

with an "optimal" data set for a large variety of research programs including the study of the fine structure of the seismic wave field. Optimal in this respect implies to record the true ground motion over a large amplitude range and a wide frequency band. The best way from a technical point of view to reach this aim is to combine broad-band seismometry with the wavenumber resolving capabilities of arrays (Baker, 1970; Berckhemer, 1971). This concept differs as well from conventional detection arrays like LASA (Green et al., 1965) as from the new SRO-installations (Peterson et al., 1976) both of which only record seismic waves in usual period bands around 1 s and 20 s.

Because of the large dynamic range of earthquake signals broad-band recording represents not only a different technical approach. It also requires a careful study of signal and noise characteristics in the total seismic frequency band.

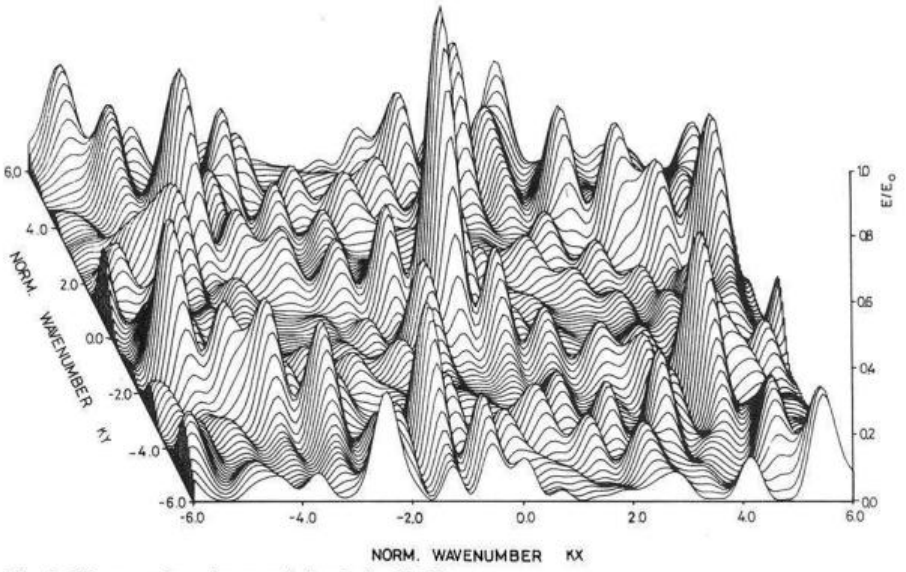

Fig. 2. Wavenumber characteristic of the GRF-array

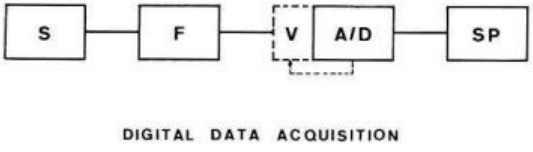

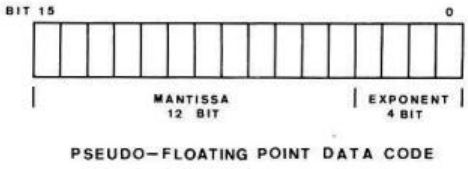

Fig. 3. Digital data aquisition and data format.
S Broad-band seismometer;
F Antialiasing filter;
V Gain-ranging amplifier;
A/D Analog-digital converter

Array Configuration

The purpose of the installation of a broad-band array is not so much to enhance signal to noise ratio rather than to set up a data base for frequency-wavenumber analysis of seismograms. In any case the success of the array concept depends on noise conditions and signal coherence. In a densely settled and highly industrialized country like Germany it is difficult to find a suitable area with homogeneous geological structure. A careful study showed that the formation of the Swabian-Frankonian Jura in Southern Germany fulfilled these conditions best.

Figure 1 shows the configuration of the GRF-array. The approximate L-shape of 80 km extension is given due to geological constraints. The array

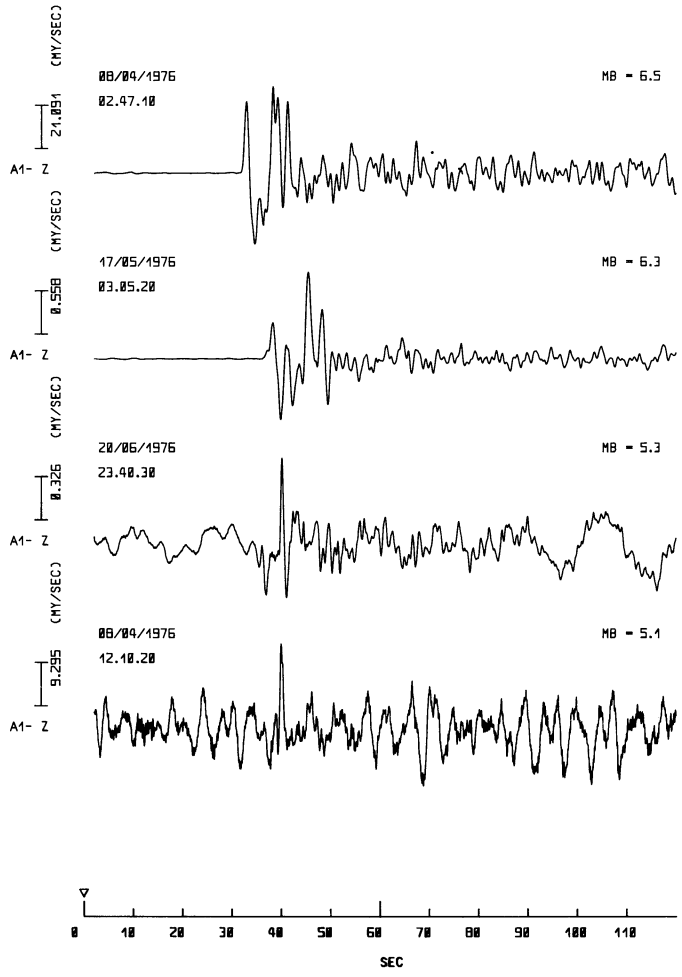

Fig. 4. Seismograms of four Uzbekistan earthquakes recorded with the GRF broad-band system

consists of 13 seismometer sites which form three triangular subarrays and some stations in between to reduce sidelobe effects in the array response. The distances between the seismometers are chosen such that the microseismic noise can be reduced by simple summation of single traces. As has been suggested (Baker, 1970) and later experimentally proven (Henger, 1975) distances of 10–12 km are suitable for broad-band recordings. Figure 2 features the array response for monochromatic signals. This is only slightly changed for broad-band inputs (Kelly, 1967). This three-dimensional wavenumber characteristic shows the rejection capability of the array as a function of wavenumber $\vec{\mathbf{k}}$ normalized to the array dimension ($\mathbf{k}_{\mathrm{NORM}}$). The width of the rejection band between the main lobe at $|\vec{\mathbf{k}}_{\mathrm{NORM}}|=0$ and the side lobes at $|\vec{\mathbf{k}}_{\mathrm{NORM}}|=6$ depends on the array size. The array shown in Figure 1 is especially designed to suppress coherent seismic noise in the medium frequency range (0.05 to 0.5 Hz) propaga-

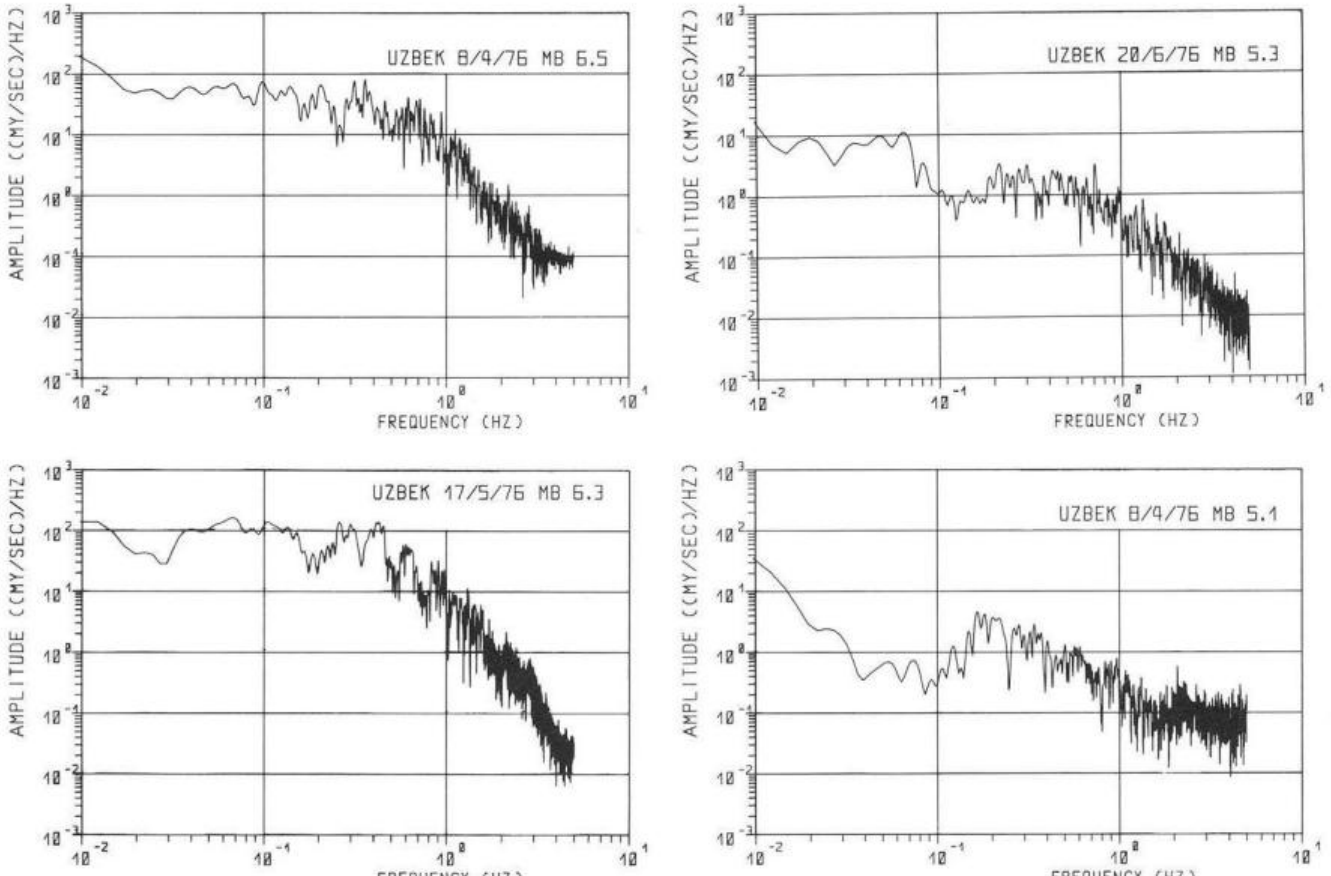

Fig. 5. *P*-wave spectra of the Uzbekistan earthquakes in Figure 4

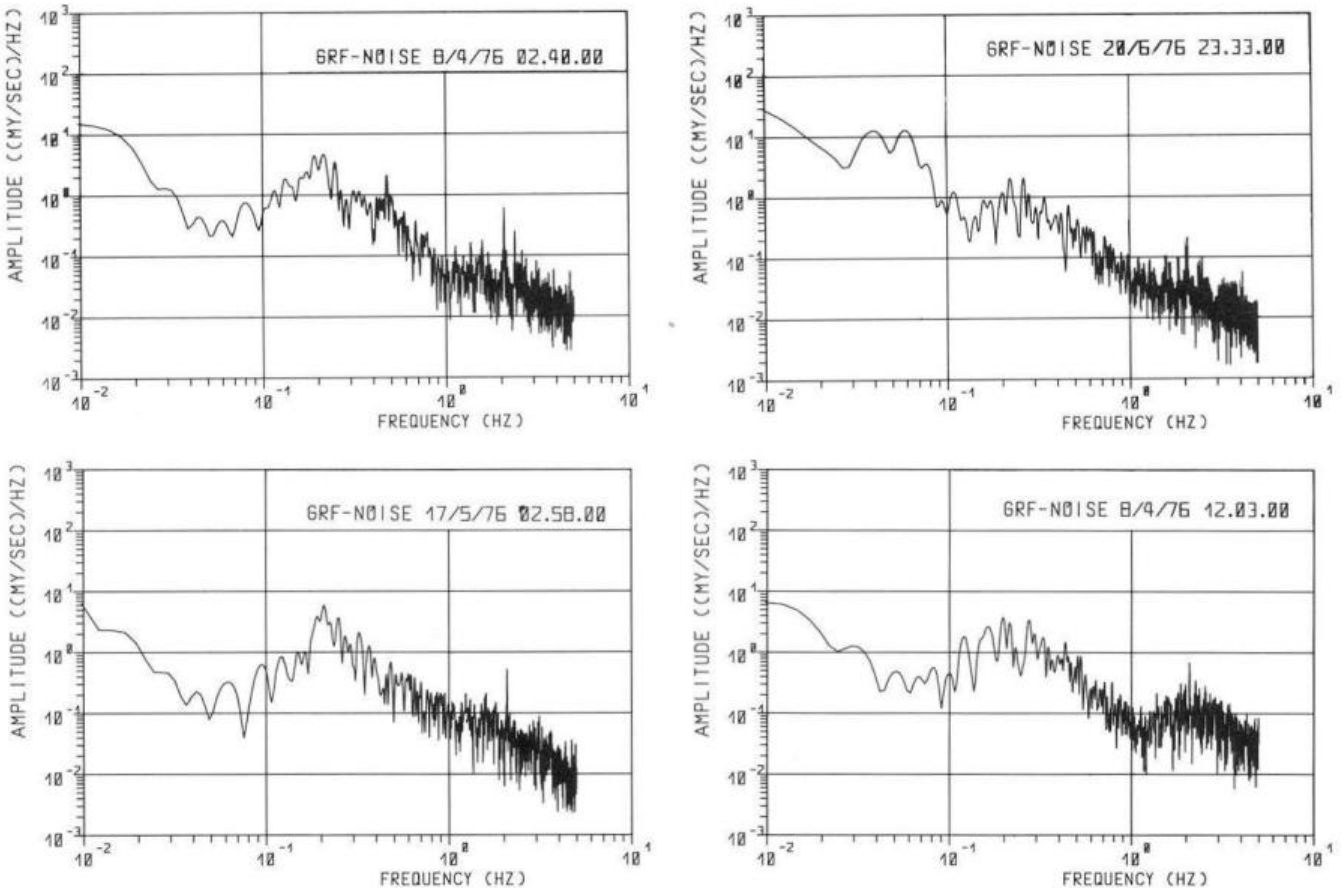

Fig. 6. Spectra of noise proceeding the signals in Figure 4

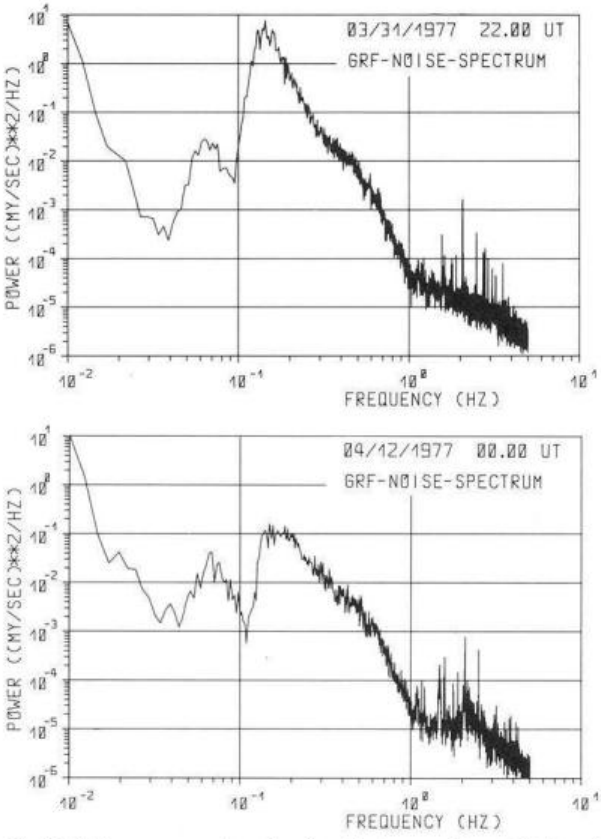

Fig. 7. Noise powerspectra showing the temporal amplitude variations of microseism at GRF

ting at surface wave velocities. The seismometer output is digitized at the site with 20 samples per second. The digital information is transmitted on telephone cables in asynchronous mode to a subarray centre which is a three-component station. The three subarrays are connected with the data centre in Erlangen by 2400 baud synchronuous lines. Technical details of the data acquisition and transmission are already published (Harjes et al., 1973), the basic principle is summarized in Figure 3 (upper half). The seismometer output passes an antialiasing filter (3db-point at 5 Hz, 42 db/octave slope) and is converted into digital form by a computerized binary gain-ranging system. In the data centre all data are stored on magnetic tapes for about one year to extract event tapes for various scientific purposes. The lower half of Figure 3 shows the data format which is a pseudo-floating point code very similar to the SRO data format (Seismic Research Observatories installed by USGS).

Test data from the first three-component broad-band station at GRF are available since 1974, the northern triangular subarray in Figure 1 is in continuous operation since April 1976 whereas the two other subarrays will be installed in 1978. The seismograms of the following chapters are examples of this data base.

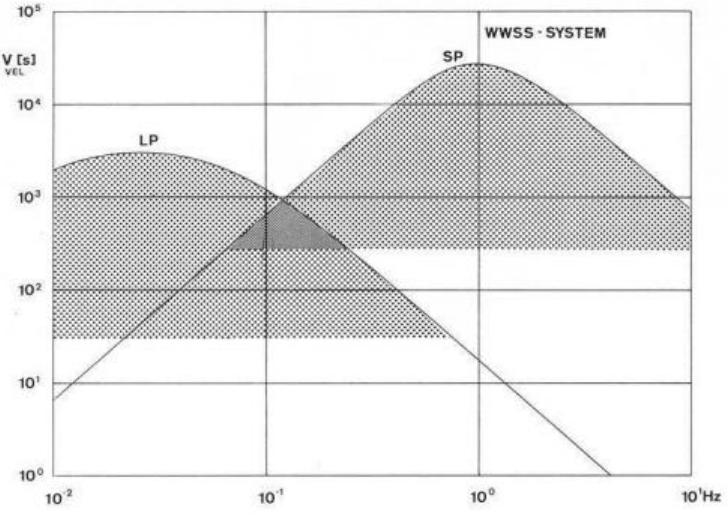

Fig. 8. Velocity response characteristic and dynamic range of short period (maximum magnification 200 k) and long period (maximum magnification 1 k) World-Wide Standard Seismographs

Seismological Implications on Broad-Band Systems

The amplitude range and frequency content of seismic signals and background noise gives very clear constrains to the instrumental realization of broad-band seismographs. Some examples of the GRF recordings will illustrate the importance of the medium frequency range between conventional long-period and short-period instrumental responses. In Figure 4 there is plotted the body wave arrival of four shallow Uzbekistan earthquakes of different magnitudes (PDE-values).

The amplitude spectra of these events are given in Figure 5 which show besides the well known trend a large variability of the maximum compressional energy and a pronounced fine structure between 0.1 Hz and 1 Hz. The quantitative interpretation of the *P*-wave spectrum is the more difficult the weaker the event is because of the influence of the microseismic noise. This is demonstrated by comparison of the noise spectra in Figure 6 computed from a noise sample just before the *P*-onset. The noise problem becomes even more important if we look at the large variability of the microseismic peak (Fig. 7) which differs by 40 db in the two examples. These broad-band noise spectra were computed by the periodogram method using 10 nonoverlapping segments each of 400 seconds length (90% confidence limit is 7 db).

Thus, two factors define the seismological data acquisition system: the dynamic range which gives the saturating point of the system, and the resolution which should be constant over a wide frequency range. Only a digital technique allows recording the total frequency and magnitude range without saturation. A binary gain-ranging concept is then adequate to get constant resolution. High resolution is needed to separate signal and noise components for spectral

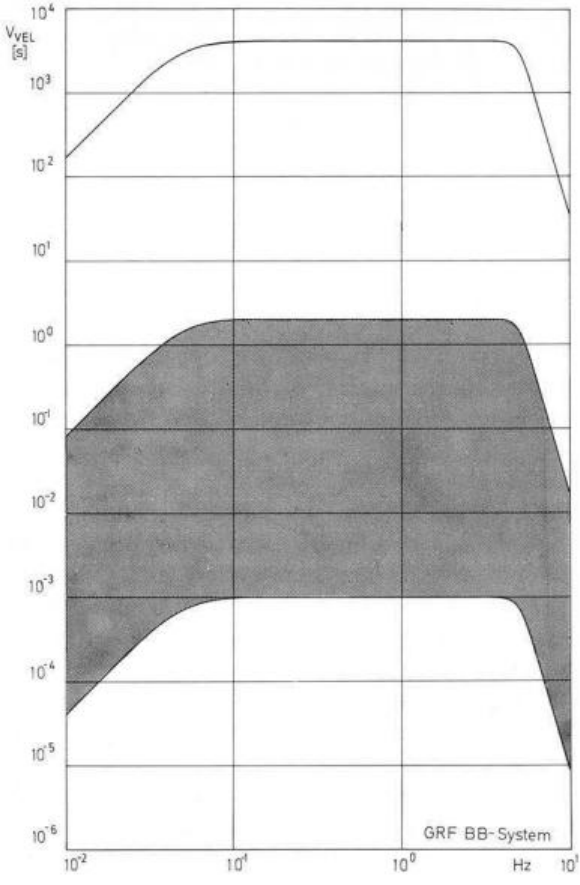

Fig. 9. Velocity response characteristic, dynamic range and resolution (shaded area) of the GRF broad-band system

analysis. In the medium frequency range where signal and noise strongly overlap the separation can only be accomplished by the use of broad-band array data.

To compare the GRF-type digital data acquisition with conventional analog seismographs the velocity response curves of the WWSSN-system are plotted in Figure 8. The corresponding maximum magnifications are 1 k for the long-period and 200 k for the short-period system. The shaded area indicates the dynamic range for direct recording. The low resolution for both systems in the medium frequency range strongly limits the numerical inversion of instrumental filtering effects. In comparison Figure 9 shows the velocity response, dynamic range and resolution for the GRF wide-band system.

During the test phase of the array a Sprengnether S-5100 seismometer was used, in the final version a new leaf-spring seismometer (Wielandt, 1975) will be installed which is of smaller size and higher stability. The seismometer acts as a high-pass filter with corner frequency at 0.05 Hz and 12 db/octave slope for the velocity response, the high frequency limitation of the transfer function is given by the antialiasing filter with a 3 db point at 5 Hz and a 42 db/octave slope.

Table 1. Comparison of GRF and WWSSN-recording systems

Resolution (1 s)		Dynamic range (20 s)	
GRF-BB	WWSSN-SP (200 K)	GRF-BB	WWSSN-LP (1 K)
1 Bit ≙ 1,2 nm/s Least significant bit	$\frac{1}{4}$ mm ≙ 9 nm/s	22 Bit ≙ 8,8 mm/s Most significant bit	15 cm ≙ 0.050 mm/s

In Figure 9 the lowest and uppermost curves limit the dynamic range of 138 db while the shaded area shows the resolution of 66 db. Because of the floating-point amplication this resolution remains constant over the whole recording range.

Table 1 compares in a different way the GRF digital system where the magnification of the recording is arbitrary with a conventional analog system with photographic registration. Assuming that in the short-period range the smallest visible amplitude is 0.25 mm and for the long-period film recording the largest amplitude is 15 cm the superiority of one single digital broad-band instrument in both frequency bands can be deduced from Table 1. In the short-period range an amplitude of 0.25 mm is equivalent to a ground velocity of about 9 nm/s. In comparison the least significant bit of the digital broad-band system represents about 1 nm/s which means a higher sensitivity by a factor of 9 than the short-period WWSSN.

Similarly for the long-period band an amplitude of 15 cm gives a saturating point at 0.05 mm/s, which demonstrates the well-known clipping problem of the long-period WWSSN. The digital broad-band system reaches its saturation point at about 1 cm/s (at 20 s).

With digital data acquisition the dynamic range of the recording system is arbitrarily high, hence the transfer function of the seismometer should be as broad as reasonable to record the true ground motion. A special instrumental characteristic which optimizes the signal/noise ratio in small frequency bands is not necessary. Thereby the restitution problem is practically avoided, and arbitrary transfer functions may be simulated by simple digital filters.

Numerical Analysis of Digital Seismic Recordings

A broad-band seismogram is an overall picture of the seismic wave field. The high dynamic range allows to focus upon special features by digital filters. These filters can simulate arbitrary seismographs or restitute the true ground motion. Figure 10 shows the mathematical formulation of the simulation for arbitrary seismometer-galvanometer combinations applying the z-form method (Kaiser, 1963). The continuous system with the transfer function $G(s)$ transforms the broad-band seismogram $x(t)$ into the simulated seismogram $u(t)$. A discrete description of this continuous transfer function is obtained by the use of the

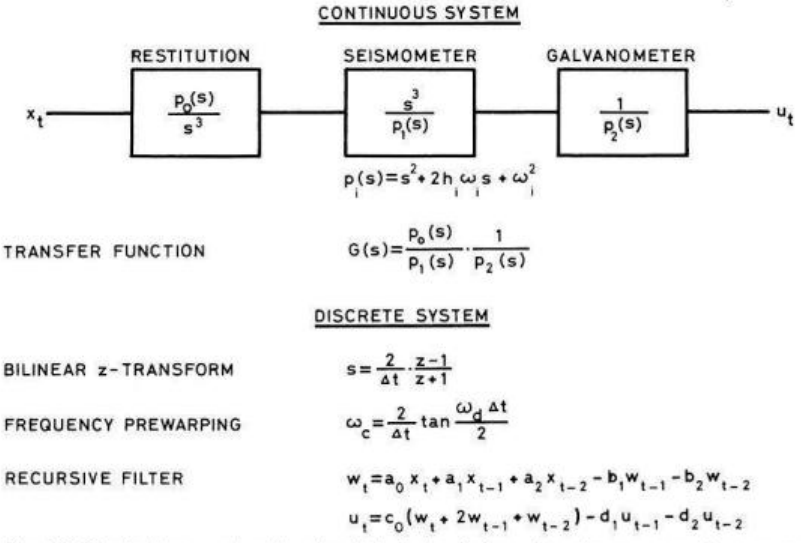

Fig. 10. Block diagram showing the digital simulation of a seismometer-galvanometer system with a double-recursive filter applying the z-form method

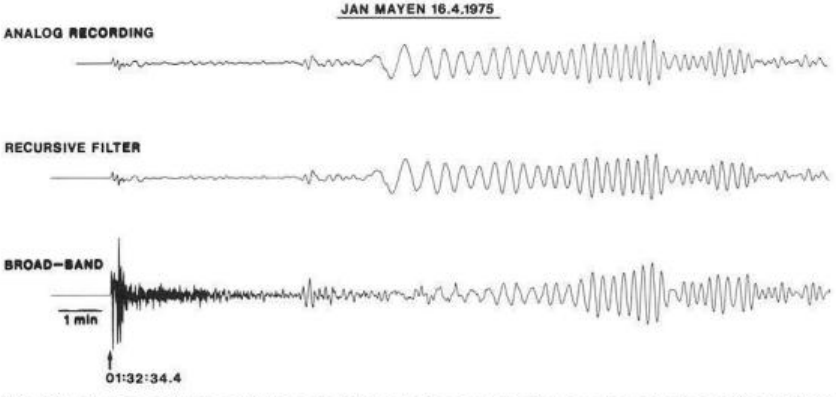

Fig. 11. Analog seismogram recorded by a long-period seismometer-galvanometer system ($T_s=20$ s, $T_g=100$ s, $h_s=h_g=1.0$) and corresponding seismogram filtered from the digital broad-band data (lowermost line) for a Jan-Mayen earthquake on April 16, 1975 (Origin Time 01:27:18.7, latitude 71.5° N, longitude 10.4° W, $m_b=6.1$)

bilinear z-transform which is ideally adapted to digital systems. The inverse transformation into the time domain yields a cascade recursive filter. The filter coefficients depend on the instrumental parameters (free period, damping) of the broad-band seismograph and the simulated seismometer-galvanometer system. A detailed description of the simulation and restitution problem for broad-band seismograms will be published in a subsequent paper.

The accuracy of the filter method is demonstrated in Figure 11. The seismogram on the bottom of this picture shows the digital broad-band recording whilst the uppermost seismogram is an analog record of a long-period seismome-

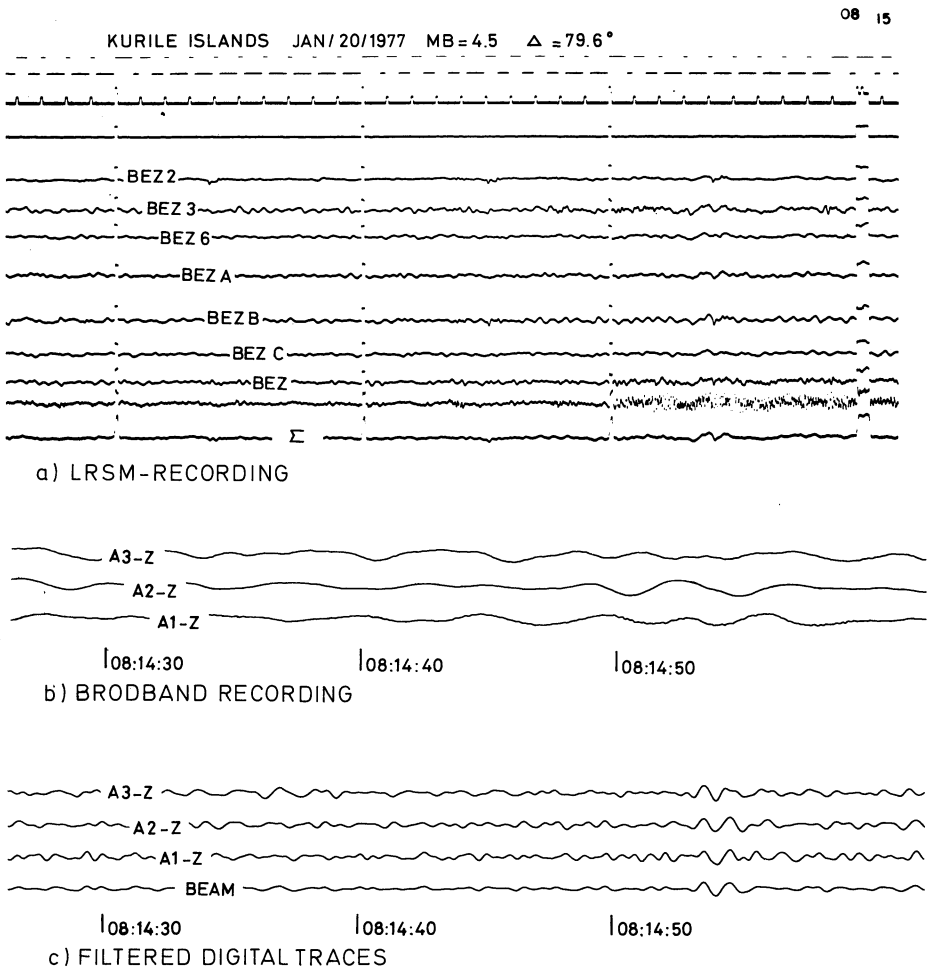

Fig. 12. a LRSM-recording at GRF of a weak teleseismic event; **b** Digital broad-band recording; **c** Digital filtered traces and beam

ter-galvanometer system ($T_s=20$s, $T_g=100$s, $h_s=h_g=1.0$). This is found to compare precisely with the digitally simulated seismogram in between both recordings.

Filtering digital broad-band seismograms can also help to avoid one particular disadvantage of conventional analog wide-band recordings, namely its poor detection capability. Figure 12a shows a small Kuril-earthquake ($m_b=4.5$) recorded with the LRSM-array at GRF. The event is near the detection level of this very sensitive instrument (maximum magnification 200 k for 0.3s, seismometer distance about 2 km). Because of the visual coherency of the *P*-onsets and a signal/noise ratio improvement in the summed trace (Σ) the event is clearly discernible. On the contrary it is hidden in the broad-band recording for the same time interval (Fig. 12b). One can use the filter technique of figure 10 to simulate the LRSM-characteristic. Figure 12c shows the result of an approxi-

mate simulation by simple band-pass filtering. The weak event is easily detected even if it is about 40 db below the noise level. There is a higher signal/noise ratio in the beam of the three instruments (lowermost seismogram) of the northern subarray (see Fig. 1) than in the summed trace of 8 analog short-period seismometers.

This example shows that broad-band instruments with floating-point amplification at least arrive at the same detection level as short-period conventional sensors. Of course the purpose of a broad-band array is to avoid the signal distortion of simple frequency filters by separating the signals with wavenumber filtering techniques. Nevertheless this new data acquisition system has demonstrated a possibility to escape the trade-off between low detection level and wide-band recording.

Conclusion

Digital broad-band data acquisition is the appropriate concept to record a wide spectral and amplitude range of teleseismic signals. The digital data base can be used to simulate arbitrary seismographs and to investigate the frequency dependence of earthquake mechanisms and path effects.

Some basic seismological parameters, like magnitude, will also get a clearer meaning by the evaluation of broad-band recordings.

Acknowledgements. The authors are indebted to their colleagues in the "GRF-Working Group", especially H. Berckhemer, for many valuable discussions. We would also like to thank W. Hanka, M. Henger, and B. Stork for preparing several figures. The GRF-array project is supported by the Deutsche Forschungsgemeinschaft (German Research Council) and the Bundesanstalt für Geowissenschaften und Rohstoffe (Federal Institute for Geosciences and Natural Resources).

References

Baker, R.G.: Suggested use of a medium-period seismograph array. Bull. Seism. Soc. Am. **60**, 1735–1737 (1970)

Berckhemer, H.. The concept of wide-band seismometry. Observ. Royal Belgique, Serie Geophys. No. **101**, 214–220 (1971)

Green, P.E., Frosch, R.A., Romney, C.F.: Principles of an experimental large aperture seismic array (LASA). Proc. IEEE **53**, 1821–1833 (1965)

Harjes, H.-P., Henger, M.: Array-Seismologie. Z. Geophys. **39**, 865–905 (1973)

Henger, M.: Wavenumber filtering of microseism with triangular arrays. NATO Advanced Study Institute Series, E: Applied Sciences No. **11**, 205 210 (1975)

Kaiser, J.F.: Design methods for sampled data filters. Proc. 1st Annu. Allerton Conf. Circuit System Theory, 221–236 (1963)

Kelly, E.J.: Response of seismic arrays to wide-band signals. Linc. Lab. Techn. Note 1967-30 (1967)

Peterson, J., Butler, H.M., Holcomb, L.G., Hutt, G.R.: The Seismic Research Observatory Bull. Seism. Soc. Am. **66**, 2049–2068 (1976)

Wielandt, E.: Astatic vertical pendulum supported by a leaf spring. J. Geophys. **41**, 545–546 (1975)

Received February 15, 1978 / Revised Version May 11, 1978